

Characterization of Pb -free “ x [Ba (Zr_{0.2}Ti_{0.8}) O₃] - (1- x) [(Ba_{0.7}Ca_{0.3}) TiO₃]” Ceramics Synthesized by Solid State Reaction Route

A THESIS SUBMITTED IN PARTIAL FULFILLMENT
OF THE REQUIREMENTS FOR THE DEGREE OF
Bachelor of Technology

in

Ceramic Engineering

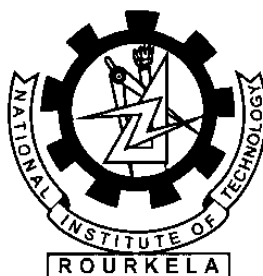
By

SUNIL KUMAR PRADHAN

(Roll No. 107CR004)

Under the guidance of

Prof. R. Mazumder



Department of Ceramic Engineering
National Institute of Technology
Rourkela-769008

2011



CERTIFICATE

This is to certify that the thesis entitled, “Characterization of Pb-free “x [Ba (Zr_{0.2}Ti_{0.8}) O₃] - (1-x) [(Ba_{0.7}Ca_{0.3}) TiO₃]”Ceramics Synthesized by Solid State Reaction Route” submitted by Mr. **Sunil Kumar Pradhan** in partial fulfillment of the requirement for the award of **Bachelor of Technology Degree in Ceramic Engineering** at National Institute of Technology, Rourkela is an authentic work carried out by him under my supervision and guidance.

To the best of my knowledge, the matter embodied in the thesis has not been submitted to any other University/ Institute for the award of any Degree or Diploma.

Date:

Prof. R. Mazumder

Dept. of Ceramic Engineering

National Institute of Technology

Rourkela-769008

ACKNOWLEDGEMENT

First and foremost I wish to offer my sincerest gratitude to my supervisor Dr R. Mazumder, Department of Ceramic Engineering, National Institute of Technology Rourkela for introducing the present topic and for his inspiring guidance, patience and valuable suggestions throughout this project work.

I must also acknowledge my gratitude to all the faculty members and staff members of Department of Ceramic Engineering, NIT Rourkela.

I am also thankful to Mr. Bhabani Sankar Sahu, Mr. Sarat kumar Rout, Mr. Abhisek Choudhary, Mr. Subrat kumar Mohanty, Tapas Mahata and other research scholars in the Department of Ceramic Engineering for providing all joyful environment in the lab and helping me out in different ways.

I would like to mention my special thanks to Mr. Ganesh kumar Sahoo, PhD scholar, Department of Ceramic Engineering for his encouragement, interest and freely given time throughout this project.

Finally, I want to say ‘thank you’ to all my batch mates for their support and valuable suggestions.

Date:

SUNIL KUMAR PRADHAN

A B S T R A C T

In the present project, x [Ba (Zr_{0.2}Ti_{0.8}) O₃] – (1- x) [(Ba_{0.7}Ca_{0.3}) TiO₃] (abbreviated as x BZT- (1- x) BCT) (where x = 0.4, 0.5, 0.6) lead-free ceramics were synthesized by conventional solid state route. XRD analysis of calcined sample shows formation of perovskite phase. The BZT- BCT ceramic samples were calcined & sintered at lower temperatures 1200⁰C and 1300⁰C, respectively which was lower compared to the previous reported literature. The average crystallite size calculated from XRD was 40 nm for 50BZT-50BCT ceramic. Dielectric measurements were carried out for the compositions over the frequency range 1Hz -1MHz and temperature range from 28⁰C to 220⁰C. Each sample showed a maximum dielectric constant at the Curie temperature (T_C). With increase in the value of ‘ x ’ from 0.4 to 0.6 the composition had shown decrease in the Curie temperature values which were 83⁰C, 77⁰C and 72⁰C respectively. The dielectric and piezoelectric properties of our sintered samples are comparable to those of conventionally prepared BZT-BCT ceramics reported earlier. These ceramics are potential candidates for the lead-free piezoelectric applications.

List of Figures

		Page no.
Fig. 1.1	Schematic representation of perovskite structure (ABO_3)	1
Fig. 1.2	Schematic for piezoelectric effect	3
Fig.1.3	(a) A cubic ABO_3 (BaTiO_3) perovskite-type unit cell and (b) three dimensional network of corner sharing octahedra of O^{2-} ions	4
Fig 2	Phase diagram of pseudo-binary ferroelectric system $[\text{Ba}(\text{Zr}_{0.2}\text{Ti}_{0.8})\text{O}_3]$ - $[(\text{Ba}_{0.7}\text{Ca}_{0.3})\text{TiO}_3]$	6
Fig 3.1	Flow chart for the powder synthesis.	11
Fig .4.1	X-ray diffraction patterns of $\text{xBZT}-(1-\text{x})\text{BCT}$ ($\text{x}= 0.4, 0.5, 0.6$) calcined at 1200°C	14
Fig. 4.2	X-ray diffraction patterns of $\text{xBZT}-(1-\text{x})\text{BCT}$ ($\text{x}= 0.4, 0.5, 0.6$) sintered at 1300°C	15
Fig.4.3	Density & shrinkage behavior of $\text{xBZT}-(1-\text{x})\text{BCT}$ ($\text{x}= 0.4, 0.5, 0.6$) ceramics sintered at 1300°C	16
Fig. 4.4.	SEM photomicrographs of polished and thermally etched (a) 50BZT-50BCT, and (b) 40BZT-60BCT ceramics sintered at 1300°C .	17
Fig. 4.5	Variation of (a) Relative permittivity (ϵ) and (b) dissipation factor with frequency of $\text{xBZT}-(1-\text{x})\text{BCT}$ ($\text{x}= 0.4, 0.5, 0.6$) ceramics.	18-19
Fig. 4.6	Temperature dependence dielectric constant of $\text{xBZT}-(1-\text{x})\text{BCT}$ ($\text{x}= 0.4, 0.5, 0.6$) ceramics.	20

List of Table

Table 1	Dielectric and piezoelectric properties of $\text{xBZT}-(1-\text{x})\text{BCT}$ ($\text{x}= 0.4, 0.5, 0.6$) ceramics.	21
---------	---	----

CONTENTS

<i>Abstract</i>		Page No
Chapter 1	GENERAL INTRODUCTION	1
	Introduction	1
1.1	Piezoelectric effect	2
1.2	Modification of Barium titanate	3-5
Chapter 2	LITERATURE REVIEW	6
2.1	Literature review	6-9
2.2	Objective of present work	10
Chapter 3	EXPERIMENTAL WORK	11
	Preparation of BZT-BCT ceramics	11-13
	General Characterization	11-13
Chapter 4	RESULTS AND DISCUSSION	14
4.1	X-ray analysis	14-15
4.2	Density & Shrinkage behavior of samples	16
4.3	SEM analysis	17
4.4	Dielectric measurement	18-20
4.5	Piezoelectric measurements at room temperature	21
Chapter 5	CONCLUSIONS, FUTURE WORK AND REFERENCES	22-25

CHAPTER - 1

GENERAL INTRODUCTION

Introduction

Barium titanate (BaTiO_3) based ceramics exhibit perovskite type of crystal structure. Perovskite oxides are the most studied ferroelectric oxide family. This large family includes ABO_3 compounds, where 'A' and 'B' are cation elements or mixture of two or more cation elements. In the ideal perovskite crystal structure, if 'A' atom is taken at the corner of the cube, then 'B' atom resides in the body centre and an oxygen atom at each face centre of the cube .[1]

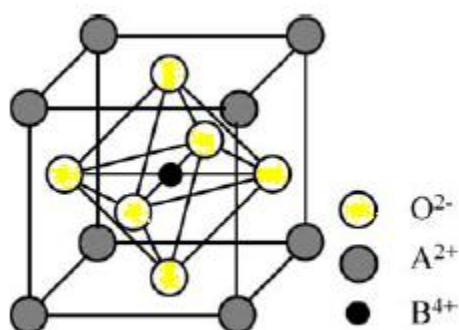


Fig.1.1 Schematic Representation of Perovskite structure (ABO_3) [2]

The chemistry of ABO_3 perovskite permits wide modifications by the way of isovalent substituent or donor dopants at A or B sites with cations of approximately matching ionic radii. This allows getting some tailor made properties by using appropriate dopants to an appropriate quantity. PZT (lead zirconate titanate) ceramics had been the most sought after perovskite oxide since last 50 years due to their superior piezoelectric and electromechanical properties. Although PZT ceramics exhibit pretty good piezoelectric constants, the manufacturing of these ceramics has been restricted due to Pb-toxicity, PbO-volatility and its hazardous effect on the environment. This is one of the reasons why barium titanate based ceramics has took the attention of researchers in recent years. Another reason is that barium titanate does not have very

good dielectric & piezoelectric properties in its pure form, but it is well known in electroceramics that doping is an effective way to get better electromechanical and physical properties [3]. Barium titanate ceramics show remarkable variation in their physical and structural characteristics with respect to ‘Ca’ and Zr’’ substitution.

For pure BaTiO₃, the permittivity passes through a maximum at 130⁰C where the long-range domain structure characteristic of the tetragonal phase vanishes and it results in high permittivity. This transition temperature is called Curie temperature (T_C). At temperatures above T_C, in the cubic paraelectric region, TiO₆ octahedra are distorted and no permanent dipoles exist. The individual dipoles give rise to Curie-Weiss relation [4]. This is as follows:

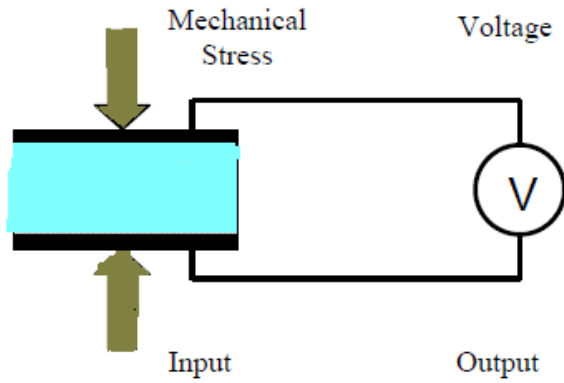
$$\frac{1}{\epsilon_r} = \frac{T - T_0}{C}, \quad T > T_C$$

Where, C = Curie-Weiss constant,

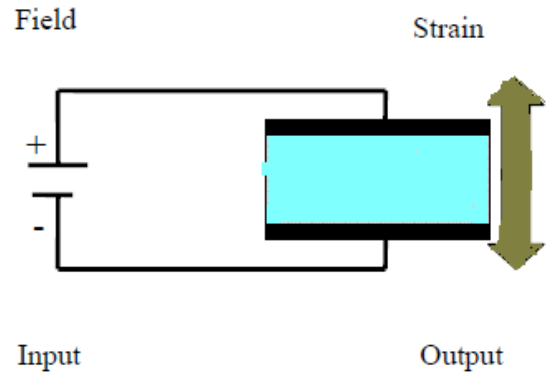
T₀=Curie-Weiss temperature.

1.1 Piezoelectric effect

All ferroelectric materials show piezoelectric effects. This phenomenon is generally of two types namely; direct and converse piezoelectric effect. In direct piezoelectric effect, on application of stress to the material, potential difference develops across the material whereas in case of converse piezoelectric effect, stress or/and strain develops in the material as a result of application of an electric field across the material [3]. Fig-1.2 explains it better.



a) Direct piezoelectric effect

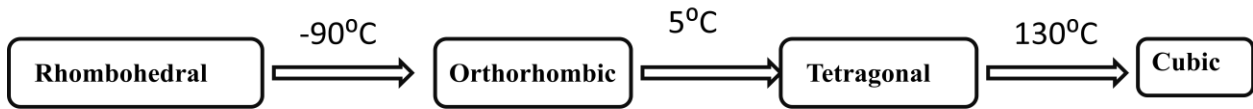


b) converse piezoelectric effect

Fig.1.2 Schematic for piezoelectric effect [3].

1.2 Modification of barium titanate

Due to its high relative permittivity and easy manufacturing process barium titanate has been the first choice to be used in multilayer ceramic capacitors (MLCCs). BaTiO_3 shows phase transitions at 130°C (cubic to tetragonal), 0°C (tetragonal to orthorhombic), -90°C (orthorhombic to rhombohedral) [5].



These phase transitions result in higher relative permittivity near the phase transition temperatures in $\epsilon_r \sim T$ curve. For ferroelectric BaTiO_3 , when more than one kind of ions reside in one of the available cation sub-lattices to form solid solution, then the normal sharp phase transition at T_C from ferroelectric to paraelectric state becomes diffused [6]. The phase transition temperatures of BaTiO_3 can be modified by partial substitution of either Ba^{2+} or Ti^{4+} . ‘Sr’ substitution for Ba decreases the T_C while ‘Pb’ substitution at Ba-sites, increases the T_C without

any considerable broadening of the phase transition [7]. With Ti-site doping, the geometry of the TiO_6 octahedra is modified which in turn, leads to the broadening of the phase transition at T_C . Substitution of Ti ions by tin or hafnium results in the reduction of T_C and an increase in the relative permittivity at ' T_C ' with respect to the amount of dopants used.

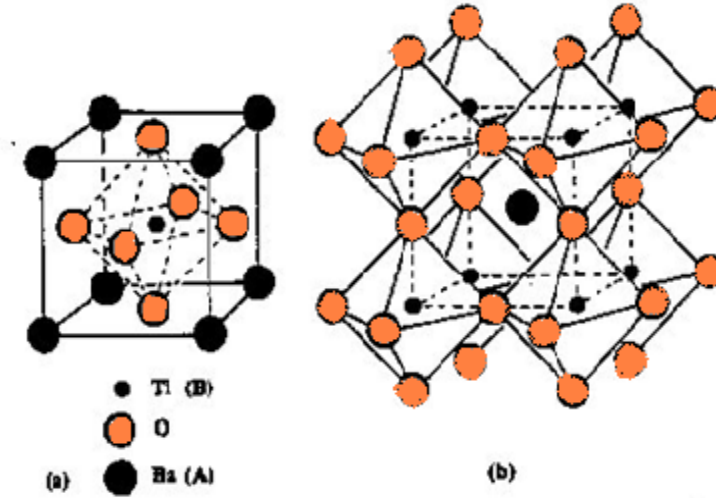


Fig 1.3 (a) A cubic ABO_3 (BaTiO_3) perovskite-type unit cell and (b) three dimensional network of corner sharing octahedra of O^{2-} ions [8].

Barium zirconate titanate ($\text{BaZr}_x\text{Ti}_{1-x}\text{O}_3$, BZT) is obtained by substituting Ti ions at B-sites of BaTiO_3 with Zr ions. This type of substitutions reduces T_C and broadens the $\epsilon_r \sim T$ curve. According to Brajer and Kulscar [9], as the Zr^{4+} content increases, the phase transition temperature of orthorhombic to tetragonal transition increases, while the tetragonal to cubic phase transition temperature decreases. As a result, for certain Zr content ($\text{Zr}/\text{Ti} > 0.1$) the three relative permittivity peaks merge into a single maximum broad peak [10]. For $\text{Zr} < 0.1\text{mol\%}$, the BZT ceramics show normal ferroelectric behaviours. When Zr content is around 27mol%, then

Zr-rich compositions show relaxor like behaviour (T_C shifts to higher temperatures with increase in frequency) [11], [12][13].

Calcium is one of the most commonly used dopants for BaTiO_3 . It has been reported that ‘Ca’ ion occupies both Ba-site and Ti-sites [14], [15], [16]. When Ca^{2+} partly substitutes Ba^{2+} , it broadens the $\epsilon_r \sim T$ curve, improves electromechanical properties and restricts the formation of the unwanted hexagonal phase of BaTiO_3 [14], [16], [17]. But there are several controversial demonstrations on the phase transition in BCT ceramics. Berlincourt and Kulesar concluded that Ca-substitution on BaTiO_3 has negligible effect [9]. Later, Mitsui and Westphal reported that Ca-substitution results in a sharp phase transition and Ca-substitution increases T_C of $(\text{Ba}_{1-x}\text{Ca}_x\text{TiO}_3)$ BCT ceramics at $x=0$ to a maximum value of 137°C at $x=0.08$ and then decreases slightly at the solid solution limit of $x=0.24$ [16]. Zhuang et al. reported that addition of even a small quantity of Ca ions at Ti-sites leads to a diffused phase transition curve and considerably lowers the phase transition temperatures [14]. However, Tiwari et al. reported that calcium doping increases the phase transition temperatures of BCT ceramics and Ba^{2+} substitution by Ca^{2+} leads to diffused transition curve. Earlier it was believed that Ca-substitution decreases the Curie temperature [18], but recently, it has been reported that Ca-doping can also increase the Curie temperature depending on the powder preparation method & the site occupancy of calcium [15]. Ca-substitution at Ba-site leads to diffuseness where as Ca replacement at Ti-site leads to sharpening of phase transition curve. Han et al. reported that in the samples with bulk composition with $(\text{Ba}+\text{Ca})/\text{Ti} > 1$, Ca^{2+} can replace Ti^{4+} [19], [20]. More interestingly, Tiwari et al. demonstrated that even Ca ions substitute Ti ions when $(\text{Ba}+\text{Ca})/\text{Ti} = 1$ for bulk compositions where the samples are prepared by dry route [16].

CHAPTER 2

LITERATURE REVIEW

2.1 Literature review

Liu et al. reported that the composition $0.5 (\text{BaZr}_{0.2}\text{Ti}_{0.8}\text{O}_3) - 0.5 (\text{Ba}_{0.7}\text{Ca}_{0.3}\text{TiO}_3)$ lies close to the tricritical point of rhombohedral, tetragonal and cubic phases. They had investigated the composition-piezoelectric constant relationship. Surprisingly, they found that the above mentioned composition showed piezoelectric constant value ($d_{33} \sim 620$ pC/N) very much comparable to the commercially available PZTs. They showed that as this composition was very close to morphotropic phase boundary (MPB), it showed a large d_{33} value [21].

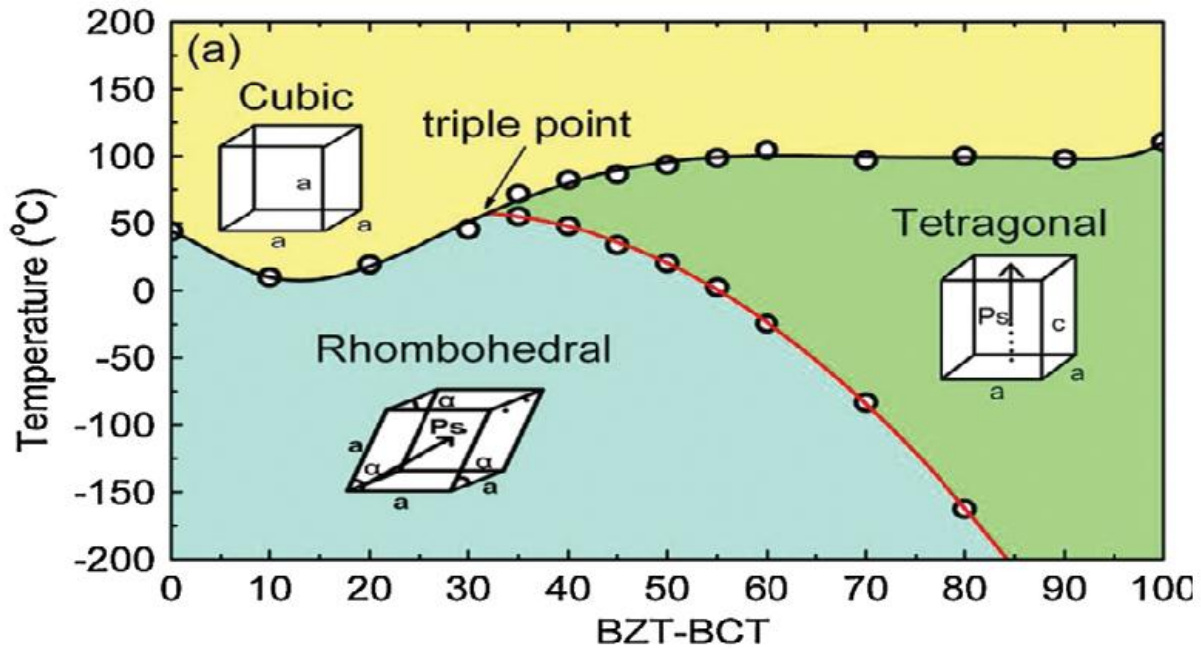


Fig 2 Phase diagram of pseudobinary ferroelectric system $\{\text{Ba} (\text{Zr}_{0.2}\text{Ti}_{0.8}) \text{O}_3\}$ - $\{(\text{Ba}_{0.7}\text{Ca}_{0.3}) \text{TiO}_3\}$ [21]

Su et al. [22] developed the composition $0.5\{\text{Ba} (\text{Zr}_{0.2}\text{Ti}_{0.8}) \text{O}_3\}$ - $0.5\{(\text{Ba}_{0.7}\text{Ca}_{0.3}) \text{TiO}_3\}$ by solid state reaction route. According to the stoichiometry of the compound, weighed quantity of BaCO_3 , CaCO_3 , TiO_2 and ZrO_2 raw chemicals were taken & mixed for 12 hours in a planetary ball mill using alcohol as medium. The resulting powder was calcined at 1350°C for 4 hours and

milled for 24 hours after that. Then the resultant powder was pressed in to disk samples by uniaxial pressing machine with 150MPa pressure. No binder was added for the compaction. Pellets prepared were sintered in the temperature range 1450⁰C-1500⁰C for 3 hours with a heating rate of 5⁰C/min. It was observed that the composition had a polymorphic phase transition between rhombohedral and tetragonal crystal structure near room temperature and a curie temperature of ~90⁰C. However, the relative permittivity had a little dependence on frequency. The value of relative permittivity at room temperature, reached a value 3000. Rhombohedral phase was the major phase in the composition with coexistence of tetragonal phase. They thought that the coexistence of phase might be the reason behind the high piezoelectric properties. The substitution of Zr for Ti, increases the polymorphic phase transition temperatures of rhombohedral -> tetragonal and orthorhombic -> tetragonal phase, but the substitution of Ca for Ba tends to decrease the transition temperatures [23],[24].

Wei Li et al. [25] prepared Pb-free BZT-BCT ((Ba_{0.93}Ca_{0.07}) (Ti_{0.95}Zr_{0.05}) O₃) compound by solid state reaction route and studied the structure and electrical properties of the compound with respect to sintering temperature. They found that BZT-BCT ceramics sintered at 1450⁰C had shown better densification, high piezoelectric co-efficient (d_{33} = 387pC/N), planar mode electromechanical coupling coefficient k_p = 44.2% and curie temperature T_C =108⁰C. They sintered the samples at 1300⁰C, 1350⁰C, 1400⁰C, 1450⁰C and 1500⁰C. From XRD analysis they found that the sample which was sintered at 1300⁰C, showed traces of rhombohedral-BaTiO₃ as a secondary phase. As the sintering temperature was increased, it showed a rapid decrease in rhombohedral-BaTiO₃ phase. This decrease could be explained by the diffusion of Ca and Zr in to the BaTiO₃ lattice to form solid solution at higher temperatures. The SEM monographs confirmed the fact that many isolated pores existed on the surface of the BZT-BCT ceramics

sintered at 1300⁰C and the average grain size was found to be below 10μm. The density of the BZT-BCT ceramics had increased with increment of sintering temperature before 1450⁰C. Further increment in sintering temperature above 1450⁰C had lowered the density observed. Two peaks were observed on the dielectric constant v/s temperature plot where the temperature was varied from 20⁰C to 140⁰C. They explained that one peak was observed because of the phase transition from orthorhombic phase to tetragonal phase and the other peak was due to phase transition from tetragonal phase to cubic phase. The transition temperatures were 38⁰C and 108⁰C respectively. They also found that the relative permittivity of the BZT-BCT ceramics had shown a rapid increase with sintering temperature and reached a maximum value of 1130⁰ at 1450⁰C(optimum sintering temperature). They concluded from their experiment that the observed high piezoelectric properties of the above compound was due to the phase transition from orthorhombic to tetragonal at around room temperature. This property increment was due to dense, uniform microstructure and stable domain alignment in polycrystalline materials.

Li et al. [26] developed lead-free (Ba_{1-x}Ca_x) (Ti_{0.9}Zr_{0.1}) O₃ ceramics with ‘x’ varying from 0.12 to 0.18 by conventional solid state reaction route. They successfully distinguished the composition range which showed the polymorphic phase transition from rhombohedral to orthorhombic at room temperature. Co-existence of both rhombohedral and orthorhombic phase at x=0.16 has increased the piezoelectric (d₃₃=328 pC/N, k_p=37.6%) and dielectric properties (ε_r=4800). Increase in ‘Ca’ content in the BZT-BCT ceramics had lowered the phase transition temperatures. They reported the effect of ‘Ca’ addition on crystal structure, microstructure, piezoelectric and dielectric properties of (Ba_{1-x}Ca_x) (Ti_{0.9}Zr_{0.1})O₃ . They prepared the BZT-BCT ceramics for x= 0.12, 0.14, 0.16, 0.18. Raw materials of BaCO₃ (99%) CaCO₃ (99%), ZrO₂ (99%), TiO₂ (99.5%) were used by them and then these were mixed with addition of ethanol &

dried and calcined at 1200°C for 4 hours. To facilitate diffusion and refining of calcined powders, the powder was again re-milled. Most importantly, the pellets were sintered at 1450°C for 4 hours in the air atmosphere. XRD patterns of the BZT-BCT ceramics had shown shifting of the positions of the diffraction peaks to higher angles with increase in calcium content.

2.2 Objective

The objective of the present work is to synthesize phase pure lead-free $x\text{Ba}(\text{Zr}_{0.2}\text{Ti}_{0.8})\text{O}_3 - (1-x)(\text{Ba}_{0.7}\text{Ca}_{0.3})\text{TiO}_3$ (BZT-BCT) ceramics (where $x=0.4, 0.5, 0.6$). The specific objectives of the present study are as follows:

- Synthesis of phase pure $(\text{Ba}_{0.88}\text{Ca}_{0.12})(\text{Zr}_{0.12}\text{Ti}_{0.88})\text{O}_3$ [60BZT-40BCT], $(\text{Ba}_{0.85}\text{Ca}_{0.15})(\text{Zr}_{0.1}\text{Ti}_{0.9})\text{O}_3$ [50BZT-50BCT], $(\text{Ba}_{0.82}\text{Ca}_{0.18})(\text{Zr}_{0.08}\text{Ti}_{0.92})\text{O}_3$ [40BZT-60BCT], [BZT-BCT] by solid state reaction route.
- To study the sintering behaviour of BZT-BCT ceramics.
- To study the dielectric property of sintered BZT-BCT ceramics.
- To study the piezoelectric coefficient of the BZT-BCT ceramic at room temperature.
- Study of SEM image analysis of the sintered pellets.

CHAPTER 3

EXPERIMENTAL WORK

Experimental Procedure

The lead free x Ba $(\text{Zr}_{0.2}\text{Ti}_{0.8})\text{O}_3$ -($1-x$) $(\text{Ba}_{0.7}\text{Ca}_{0.3})\text{TiO}_3$ (BZT-BCT) ceramics (where $x=0.4, 0.5, 0.6$) have been prepared solid state reaction technique. Reagent grade; BaCO_3 (99%), CaCO_3 (99%) and ZrO_2 (99.9%), TiO_2 (99.9%) were used as the starting material. The stoichiometric amounts of starting materials were weighted and transferred into a planetary milling pot which is filled with the ZrO_2 balls. They were milled 10 h using isopropanol as the medium. After the milling the slurry was dried at oven. Then mixture was calcined at 1200°C for 2h in an alumina crucible. The resulting powders were mixed thoroughly 3Wt% PVA binder solution and then uniaxial pressing at a pressure of 4 ton with dwelling time 120 min into a disc samples. The disc samples were finally sintered at 1300°C for 4h in air. The flow chat of the powder synthesis is given in fig 3.1.

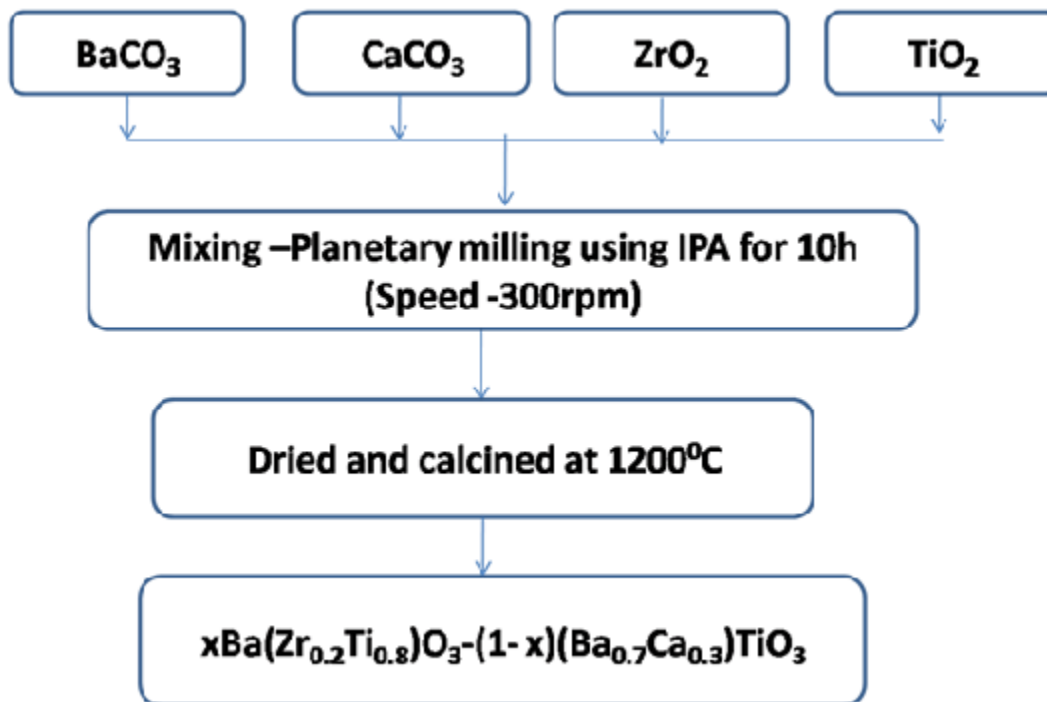


Fig 3.1 Flow chart for the powder synthesis.

The phase evolution of calcined powder as well as that of sintered samples was studied by X-ray diffraction technique (Philips PANalytical, The Netherlands) using Cu K α (0.154nm) radiation. The generator voltage and current was set at 35 KV and 25 mA respectively. The samples were scanned in the 2 θ ranges 15 $^{\circ}$ to 70 $^{\circ}$ range in continuous scan mode. The scan rate was 0.025 $^{\circ}$ /sec. Phases present in the sample has been identified by the search-match facility available with Philips X'Pert High Score Software.

The crystallite size of the calcined powders was determined from X-ray line broadening using the Scherrer equation

$$t = \frac{0.9\lambda}{B\cos\theta}$$

Where, t = crystallite size, λ = wavelength of the radiation, θ = Bragg's angle and B = full width at half maximum.

Microstructure of sintered pellets were studied by using Scanning Electron Microscope (JEOL - JSM 6480LV). The generator voltage was 15 kV. Polished samples were prepared by polishing the samples against emery paper and polished samples were washed with acetone by using an ultrasonic cleaner to remove the sample debris. The polished surface of the sample was then thermally etched at 1000 $^{\circ}$ C below the sintering temperature for 30 minutes.

Measurement of density by Archimedes principle

The bulk density of the sintered pellets was determined by Archimedes principle. The apparent porosity and bulk density were calculated as follows:

Dry weight of the sample = W_d ,

Soaked weight of the sample = W_s ,

Suspended weight of the sample = W_a

$$\text{Apparent Porosity(\%)} = \frac{W_s - W_d}{W_s - W_a} \times 100$$

$$\text{Bulk Density} = \frac{W_d}{W_s - W_a} \times \text{density of liquid medium}$$

Liquid medium used was kerosene and its density 0.781112 gm/cc

For dielectric measurement, samples have been prepared by electroding with silver paste. The silver paste coated samples were cured at 500⁰C for 30min. Dielectric measurement was carried out using **Solatron 1296**. The frequency range for dielectric measurement was varied in the range of 1 Hz to 1MHz. Dielectric measurement has also studied as a function of temperature. The piezoelectric properties were measured using a quasistatic piezoelectric constant testing meter for the samples that were poled under .5 kV/mm to 1.5kV/mm bias at room temperature in a silicone oil bath for 30 min.

CHAPTER 4

RESULTS AND DISCUSSION

Results and Discussion

4.1 X-ray analysis

Fig.4.1 shows the X-ray diffraction patterns of the $x\text{BZT}-(1-x)\text{BCT}$ ($x= 0.4, 0.5, 0.6$) powder calcined at 1200°C . It can be observed that all ceramics show pure perovskite structure, and suggesting that the Ca & Zr has diffused into the BaTiO_3 lattice side to form a solid solution. Moreover, it is clear that the position of diffraction peaks of the BZT-BCT has shifted to higher angle with increase in Ca content [27] and decrease in the Zr content. No secondary peak was found in all the BZT-BCT ceramics.

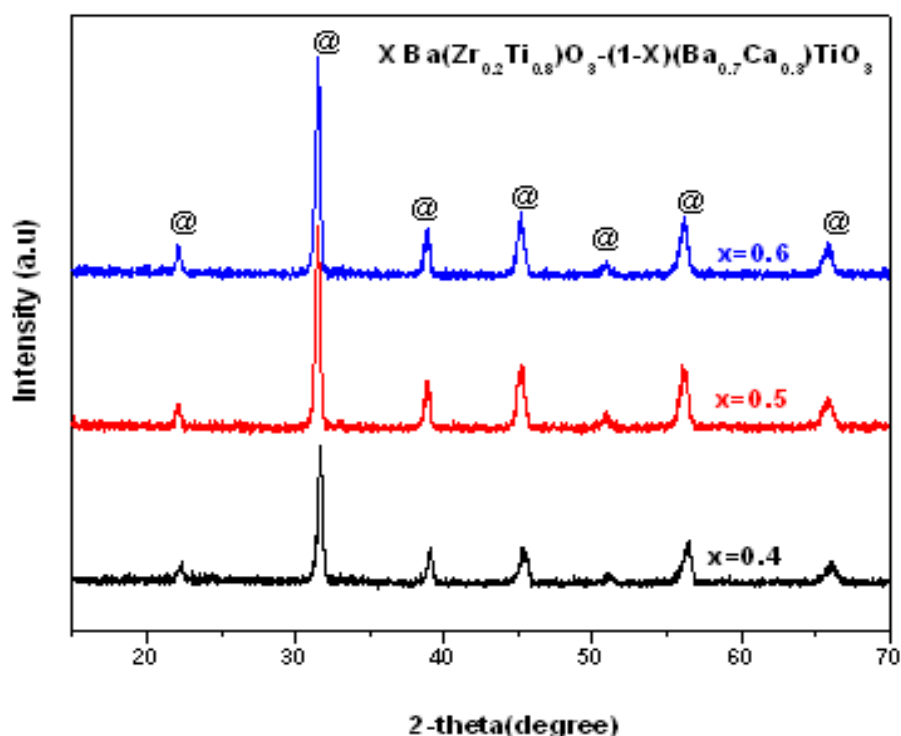


Fig .4.1 X-ray diffraction patterns of $x\text{BZT}-(1-x)\text{BCT}$ ($x= 0.4, 0.5, 0.6$) calcined at 1200°C

The average crystallite size was calculated from scherrer formula for 50BZT-50BCT , it was found to be 40nm. The BZT-BCT ceramic possessed dominant tetragonal crystal structure and it was matched with JCPDS card no 75-2119.

Fig.4.2. shows the X-ray diffraction patterns of the sintered $x\text{BZT}-(1-x)\text{BCT}$ ($x = 0.4, 0.5, 0.6$) ceramics. All BZT-BCT ceramics were sintered at 1300°C which was lower than previous reports on BZT-BCT []. All samples show the perovskite structure except 40BZT-60BCT sample.

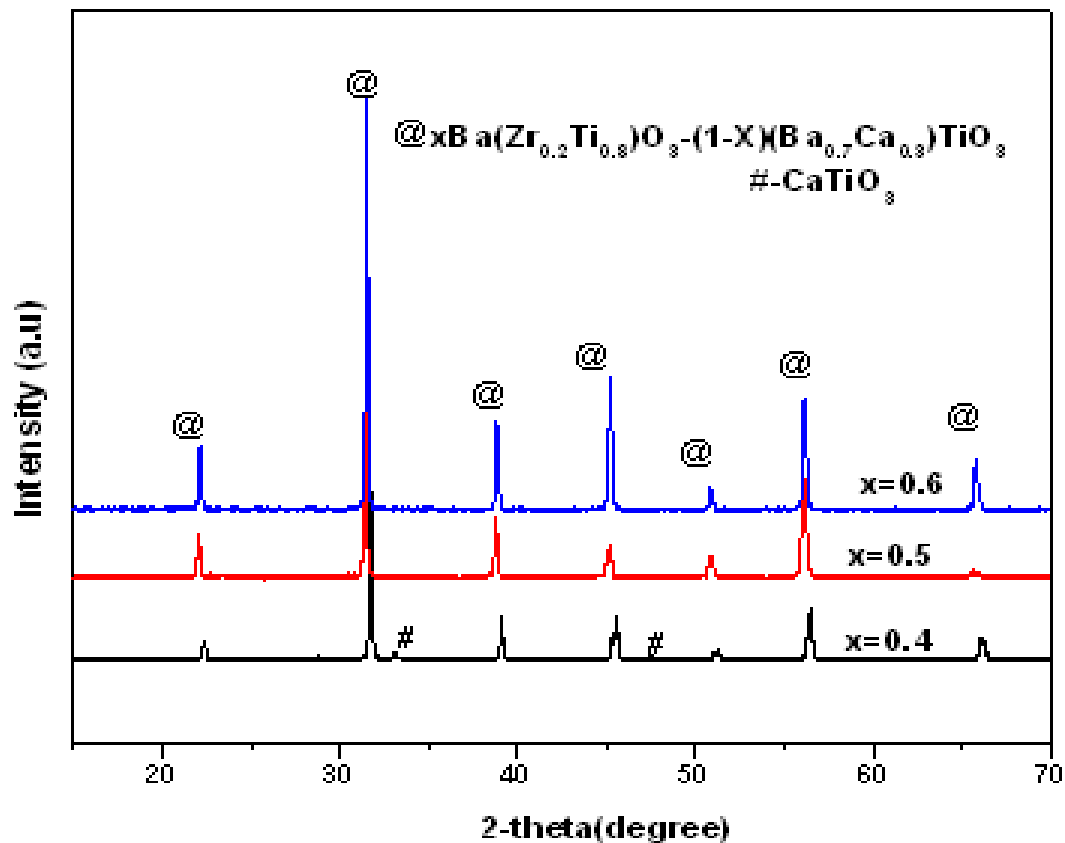


Fig. 4.2 X -Ray diffraction patterns of $x\text{BZT}-(1-x)\text{BCT}$ ($x = 0.4, 0.5, 0.6$) ceramics sintered at 1300°C

The 40BZT-60BCT samples show small impurities phase like CaTiO_3 with JCPDS card no. 810561. As the 'Ca' content increases above 15 mol%, the precipitation of second phase (CaTiO_3) starts [28]. This is a clear indication that Zr^{4+} and Ca^{2+} systematically dissolved in

BaTiO₃ lattice with homovalent substitution of Ti⁴⁺ (ionic radius 0.068 nm) by Zr⁴⁺ (ionic radius 0.079 nm) and Ba²⁺ (ionic radii .161 nm) by Ca²⁺ (ionic radius 0.134 nm) to form a homogeneous solid solution having tetragonal symmetry.

4.2. Density & Shrinkage behavior of samples

Fig 4.3 shows the density behavior of xBZT-(1-x)BCT (x= 0.4, 0.5, 0.6) ceramics sintered at 1300⁰C, it was found that density increases with increase the Ca content. The highest density was achieved in 50BZT-50BCT ceramic is 5.72gm/cc which is about > 99 % of relative density. The Shrinkage behavior of BZT-BCT ceramics are increases with increase Ca content. It observed that Maximum Shrinkage gives more density of BZT-BCT samples. Density is strongly depending upon the Ca content.

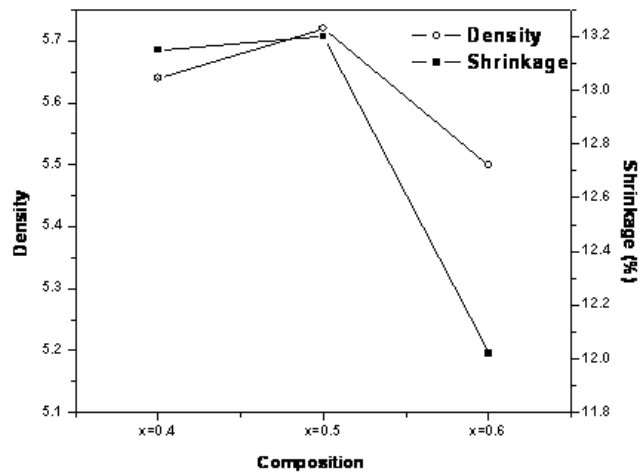


Fig.4.3 Density & shrinkage behavior of xBZT-(1-x)BCT (x= 0.4, 0.5, 0.6) ceramics sintered at 1300⁰C.

4.3 SEM image analysis of sintered BZT-BCT ceramics

The microstructure of the BZT-BCT ceramics was investigated by SEM. The micrographs clearly show that the sintered samples have dense structure with non-uniform grain size distribution. The microstructure of sintered samples depends on the method of preparation as well as the Ca-content and Zr-content. Larger contents of Ca substitution yields smaller grain size.

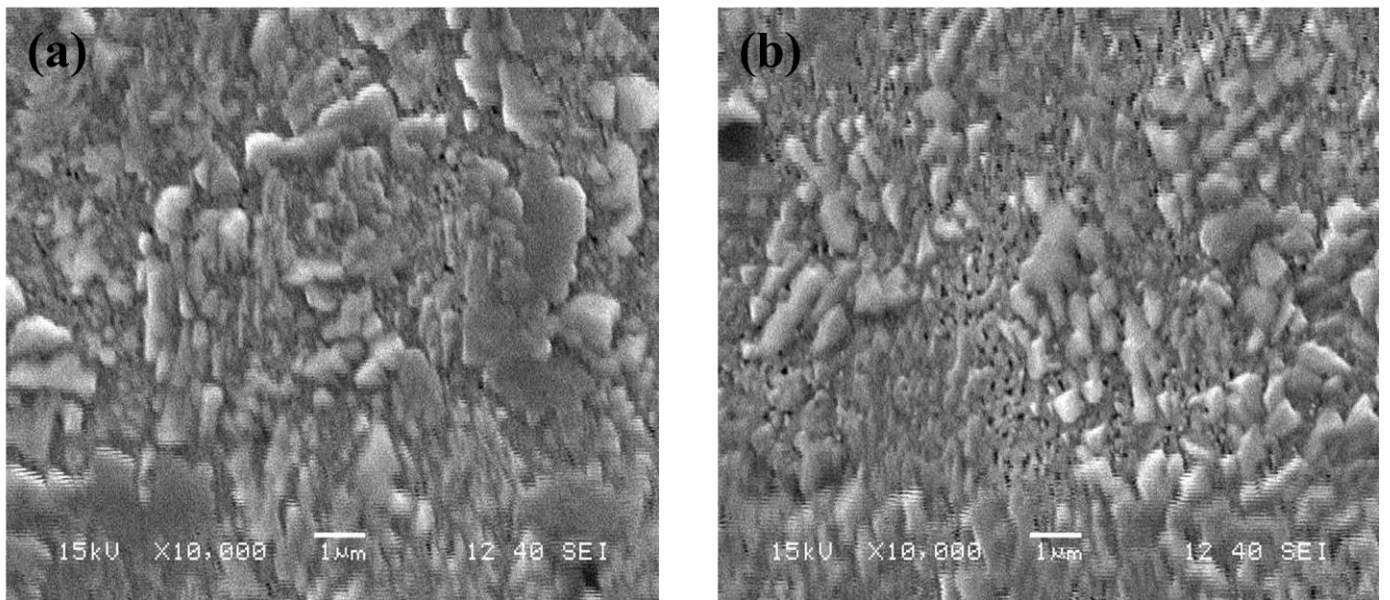
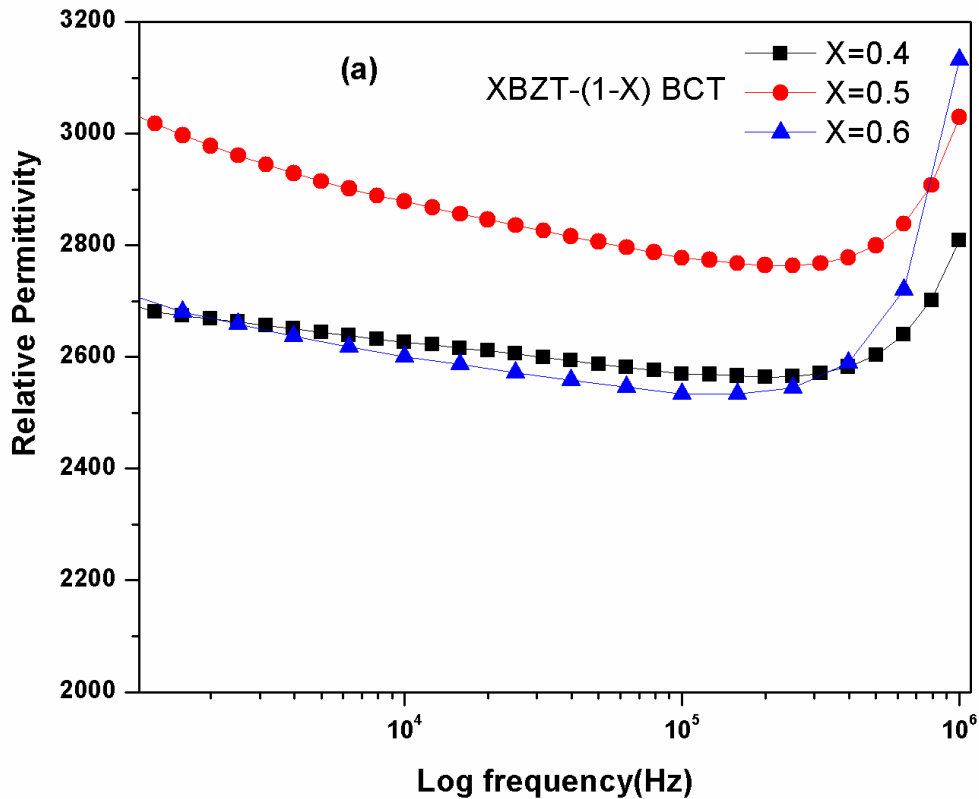


Fig. 4.4. SEM photomicrographs of polished and thermally etched (a) 50BZT-50BCT , and (b) 40BZT-60BCT , sintered at 1300⁰C.

4.4. Dielectric Measurement

4.4.1 Dielectric Measurement with frequency

The frequency dependence of relative permittivity and dissipation factor of BZT-BCT ceramics at room temperature is shown in Fig 4.5 (a) & (b). In all the samples, relative permittivity (ϵ_r) was decreasing with increase in frequency up to 400 kHz then the permittivity value increases. The relative permittivity is strongly depending upon the Ca and Zr content. The maximum relative permittivity is observed at 50BZT-50BCT ceramic. The relative permittivity values at 1 KHz are 2700, 3058, & 2712 for 40BZT-60BCT, 50BZT-50BCT & 60BZT-40BCT ceramics respectively at room temperature. The dissipation factor has decreased with increasing frequency up to 400 KHz and then it increases.



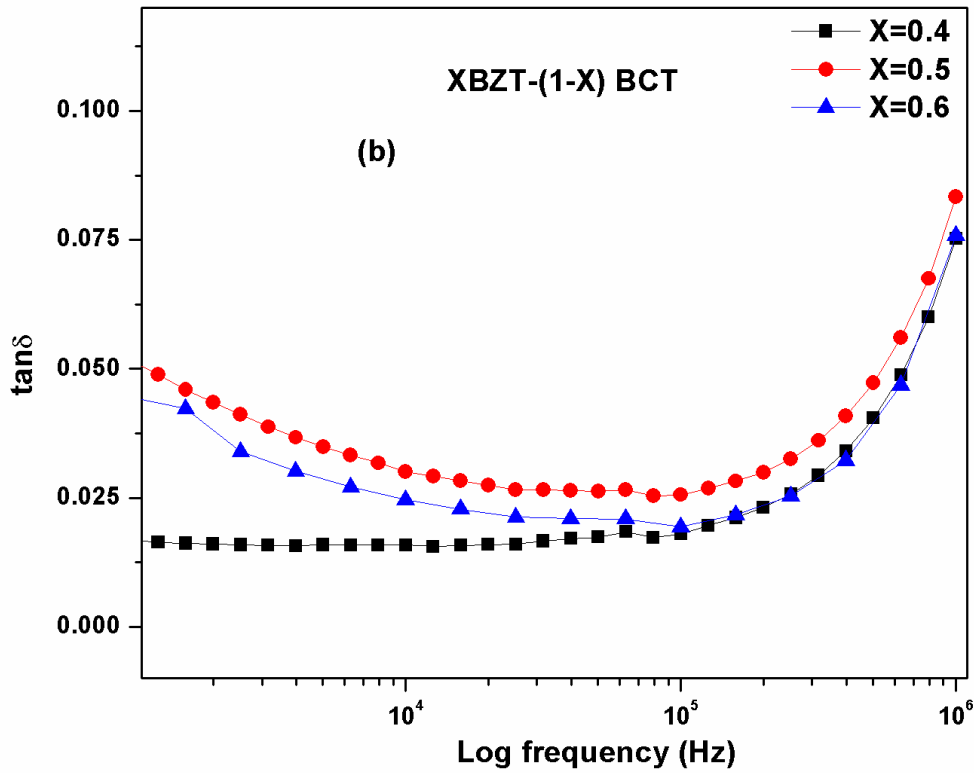


Fig. 4.5 Variation of (a) Relative permittivity (ϵ) and (b) dissipation factor with frequency of $\text{xBZT}-(1-\text{x})\text{BCT}$ ($\text{x}=0.4, 0.5, 0.6$) ceramics.

4.4 .2 Dielectric measurement with Temperature

Fig 4.6 shows the temperature dependence of dielectric constant measured at 1 kHz for $\text{xBZT}-(1-\text{x})\text{BCT}$ ($\text{x}=0.4, 0.5, 0.6$) ceramics. The highest permittivity ($\epsilon_r = 8142$) at Curie peak is observed for the 50BZT-50BCT ceramic at 1 kHz. It can be observed that all BZT-BCT ceramics have broad peak at around Curie temperature.

The Curie temperature reduced with the increase in Zr content and decreasing in Ca content due the changes in crystal structure. Addition of Zr^{4+} substituent has more prominent effect on T_C

than addition of Ca^{2+} . A small increment in Zr^{4+} addition lowers the T_C more rapidly than that of Ca^{2+} addition [11]. The Curie temperature are found 83°C , 77°C and 72°C for 50BZT-50BCT, 40BZT-60BCT and 60BZT-40BCT ceramics respectively.

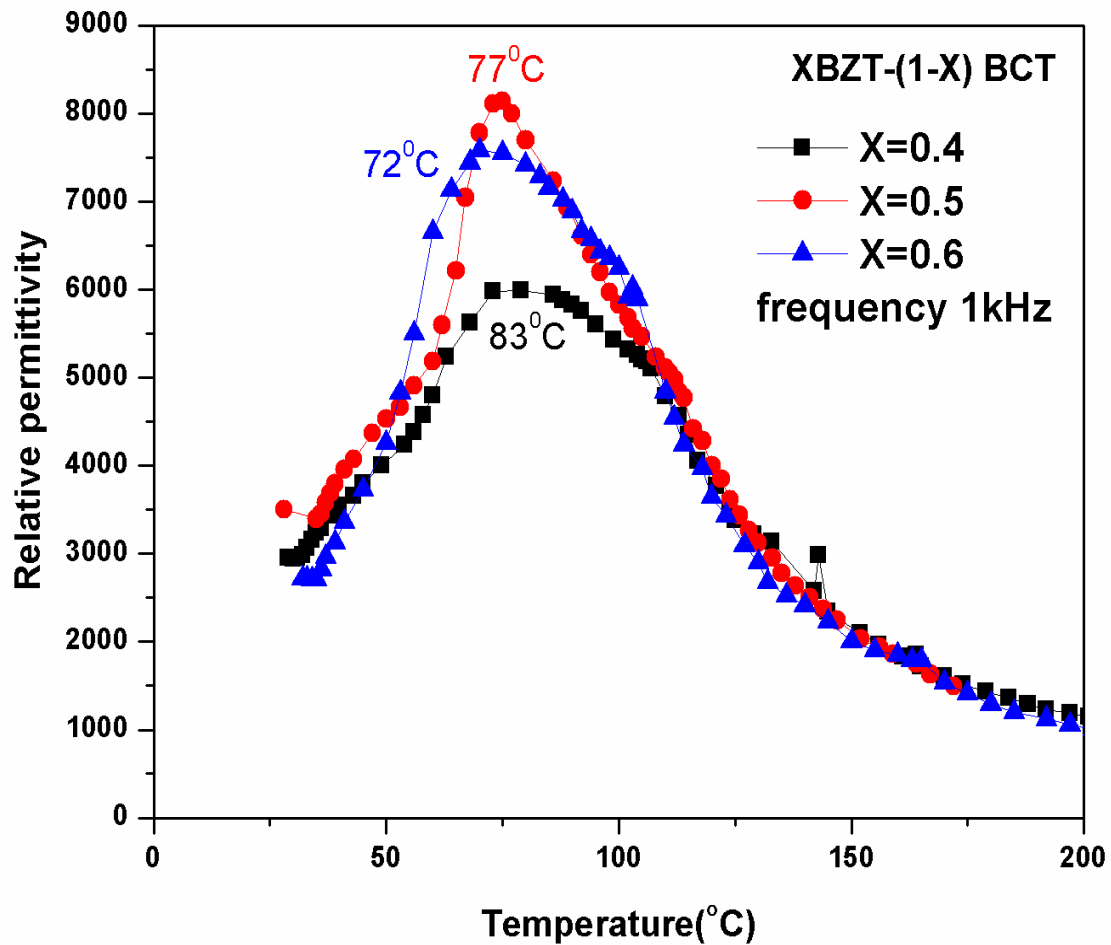


Fig. 4.6 Temperature dependence dielectric constant of $x\text{BZT}-(1-x)\text{BCT}$ ceramics where ($x= 0.4, 0.5, 0.6$).

4.5 Piezoelectric measurements at room temperature

The optimum poling field for BZT-BCT ceramics is about ~ 1.5 kV/mm and the maximum piezoelectric properties are shown in the temperature range of 30°C - 40°C [26]. As the composition 50BZT-50BCT lies close to the tri-critical point of rhombohedral, tetragonal, and cubic phases where the domain orientation is easier during poling, it shows higher d_{33} values than other two compositions. The d_{33} value of 40BZT-60BCT is also higher than that of 60BZT-40BCT [21].

Table- 1 Dielectric and piezoelectric properties of BZT-BCT ceramics

composition	Calcination temperature	Sintering temperature	Density	Dielectric properties at 1kHz	Loss factor	Piezoelectric properties(d_{33}) Poling field 1.5 kV/mm
60BZT-40BCT	1200°C	1300°C	5.5	2712	0.02	124 pC/N
50BZT-50BCT	1200°C	1300°C	5.72	3040	0.04	340 pC/N
40BZT-60BCT	1200°C	1300°C	5.64	2700	0.02	280 pC/N

CHAPTER - 5

CONCLUSIONS, FUTURE WORK
AND REFERENCES

Conclusions:

The lead-free x Ba $(\text{Zr}_{0.2}\text{Ti}_{0.8})\text{O}_3-(1-x)(\text{Ba}_{0.7}\text{Ca}_{0.3})\text{TiO}_3$ (BZT-BCT) ceramics (where $x=0.4, 0.5, 0.6$) have been prepared by solid state reaction technique. Pure phase BZT-BCT powder can be obtained at lower calcination temperature of 1200°C . XRD study of BZT-BCT ceramics indicates the pure perovskite phase with no impurity phases. Density, dielectric and piezoelectric properties were highest for 50BZT-50BCT ceramics. For 50BZT-50BCT ceramics, the d_{33} value was found to be 340pC/N . By increasing the Zr & Ca addition, a shift of Curie temperature towards room temperature takes place. The Curie temperature is found to be 83°C , 77°C and 72°C for 40BZT-60BCT, 50BZT-50BCT and 60BZT-40BCT ceramics respectively. These ceramics are potential candidates for the lead-free piezoelectric applications.

Future work:

- Detail study of piezoelectric properties of BZT-BCT ceramics.
- Detail study of Microstructure analysis of BZT-BCT ceramics.
- Study of electromechanical coupling coefficient and ferroelectric hysteresis (P-E) loop of BZT-BCT ceramics.

REFERENCES

- [1] T. Morita, Y. Cho: Appl. Phys. Lett 88, 379(2006).
- [2] D. Berlincourt, Journal Acoustic Society of America, 91(1992).
- [3] Jona F and Shirane G, Ferroelectric crystals (New York: Dover). 1993.
- [4] A. R. West, T. B. Adams, F. D. Morrison, and D.C. Sinclair, Novel high capacitance materials: BaTiO₃: La and CaCu₃Ti₄O₁₂, J. of the European Ceramic Society, 24, 1439–1448(2004).
- [5] T. Bongkarn, N. Phungjitt, N.Vittayakorn Phase formation and microstructure of Ba(Zr_{0.2}Ti_{0.8})O₃ ceramics prepared via solid state reaction method, J. of microscopy society of Thailand, 22, 30-33(2008).
- [6] J.N. Lin, T.B. Wu, Effect of isovalent substitutions on the lattice softening and transition character of BaTiO₃ solid solutions, J. Appl. Phys, **68**, 985–993(1990).
- [7] H. Nemoto, I. Oda. Dielectric examinations of PTC action of single grain boundaries in semiconducting BaTiO₃ ceramic, J.Am. Ceram.Soc. 63, 398-401(1980).
- [8] D. Hennings, H. Schell, and G. Simon, J. Am. Ceram. Soc., 65, 539–544 (1982).
- [9] DA Berlincourt, F. Kulesar, Electrochemical properties of BaTiO₃ compositions showing substantial shifts in phase transition points, J. Acoust. Soc. Am. 24, 709(1959).
- [10] A.Outzourhit, M. I. Raghni, M.L.Hafid and F.Bensamka, Journal of Alloys and Compounds 340, 214-219(2002).
- [11] X.G. Tang, Q.X. Liu, J.Wang and W. Chan, Appl. Phys A 96, 945–952 (2009).
- [12] N. Nanakorn, P. Jalupoom, N. Vaneesorn, A. Thanaboonsombut Ceramics International 34, 779–782 (2008).

- [13] W. Li, Z. Xu, R.Chu, P Fu, and G. Zang, Dielectric and piezoelectric properties of $\text{Ba}(\text{Zr}_x\text{Ti}_{1-x})\text{O}_3$ lead-free ceramics, *Brazilian Journal of Physics*, 40, 353(2010).
- [14] ZQ Zhuang, MP Harner, DM Smyth., The effect of octahedrally co-ordinated calcium on the ferroelectric transition of BaTiO_3 . *Mat. Res. Bull* 22, 1329(1987).
- [15] VS Tiwari, D Pandey, P Groves, The influence of powder processing technique on chemical homogeneity and the diffused phase transition behaviour of $\text{Ba}_{0.9}\text{Ca}_{0.1}\text{TiO}_3$ ceramics., *J Phys. D* 22 837 (1989).
- [16] P. Krishna, D. Pandey, V. Tiwari, R. Chakravarthy, and B. Dasannacharya, Effect of powder synthesis procedure on calcium site occupancies in barium calcium titanate: a rietveld analysis. *Appl. Phys. Lett.*, 62,231(1993).
- [17] T. Mitsui, Westphal Dielectric and X-ray studies of $\text{Ca}_x\text{Ba}_{1-x}\text{TiO}_3$ and $\text{Ca}_x\text{Sr}_{1-x}\text{TiO}_3$. *Phys Rev* 124,1354(1961).
- [18] A.J. Moulson, J.M. Herbert, *Electro-ceramic materials: Properties and Applications*, Chapman and Hall, London, NY(1990).
- [19] Y. H. Han, J. B. Appleby, and D. M. Smyth, *J. Am. Ceram. Soc.*, 70, 96(1987).
- [20] H. N. Chan, M. P. Harmer, M. Lal, and D. M. Smyth, *Mater. Res. Soc.Symp. Proc.* 31, 345(1984).
- [21] Wenfeng Liu and Xiaobing Ren, Large Piezoelectric Effect in Pb-Free Ceramics, *Phys. Rev. Lett.* 103, 257602 (2009).
- [22] S.Su, R. Zuo, S.Lu, Z. Xu, X. Wang and L. Li, Poling dependence and stability of piezoelectric properties of $\text{Ba}(\text{Zr}_{0.2}\text{Ti}_{0.8})\text{O}_3$ -($\text{Ba}_{0.7}\text{Ca}_{0.3}$) TiO_3 ceramics with huge piezoelectric co-efficient, *current applied physics*, In Press 1-4(2011).
- [23] B. Jaffe, W.R. Cook, H. Jaffe, *Piezoelectric Ceramics*, Academic Press, London(1971).

- [24] M.C. McQuarrie and F.W. Behnke. *J. Am. Ceram. Soc.* **37**, 539 (1954).
- [25] Wei Li, Zhijun Xu, Ruiqing Chu, Peng Fu, High piezoelectric d_{33} coefficient of lead-free $(\text{Ba}_{0.93}\text{Ca}_{0.07})(\text{Ti}_{0.95}\text{Zr}_{0.05})\text{O}_3$ ceramics sintered at optimal temperature, *Materials Science and Engineering B*, In Press (2010).
- [26] W. Li, Z. Xu, R.Chu, P Fu, and G. Zang, Polymorphic phase transition and piezoelectric properties of $(\text{Ba}_{1-x}\text{Ca}_x)(\text{Ti}_{0.9}\text{Zr}_{0.1})\text{O}_3$ lead-free ceramics, *Physica B* 405, 4513–4516 (2010).
- [27] W. Li, Z. Xu, R.Chu, P Fu, and G. Zang, Piezoelectric and Dielectric Properties of $(\text{Ba}_{1-x}\text{Ca}_x)(\text{Ti}_{0.95}\text{Zr}_{0.05})\text{O}_3$ Lead-Free Ceramics, *J. Am. Ceram. Soc.*, 93 [10] 2942–2944 (2010).
- [28] M. Yoon, S. Un, Effects of A-site Ca and B-site Zr substitution on dielectric properties and microstructure in tin-doped BaTiO_3 – CaTiO_3 composites, *Ceramics International* 34, 1941–1948 (2008).